scientific reports

Check for updates

OPEN

The influence of human activities on the microbial community structure and function of a karst cave in southwest China

Meiqi Zhang[1], Kun Luo[2], Dehua Liu[1], Yancheng Li[1,3]✉, Qian Liu[1] & Jiang Li[1,3]

With human activities like exploration, geological investigation and tourism, the structure and function of karst cave microbial communities are prone to change. In this study, sediments from seven different spots in the Dushan Tian Cave in Guizhou Province, China were collected. And the structure and potential key metabolic functions of the microbial community were analyzed through metagenomics. The results showed that the structure of the microbial communities was associated with human-impacted environmental factors. Total phosphorus and Sulfide might promote the growth of *Gemmatimonadetes_bacterium*. However, Sulfide and organic matter might inhibit the growth of Gemmatimonadetes, *Gemmatimonadetes_bacterium*, Acidobacteria and *Candidatus_Rokubacteria*. Human activities triggered ecological effects. In terms of the abundance, denitrification genes increased but ammonia oxidation genes decreased in nitrogen metabolism, suggested there was an increasing trend in the potential of denitrification function. The sulfur metabolic potentials mainly involved assimilatory sulfate reduction where sulfates might be accumulated. The potential of carbon metabolism showed a trend towards the decomposition of exogenous carbon. The methane potential had changed. This study revealed the impact of human activities on cave microorganisms and clarified the response mechanism of cave microorganisms under human interference. It provided an important reference for the ecological protection and development and utilization of karst caves.

Keywords Dushan Tian Cave, Sediments, Environmental factors, Microbial community structure, Metabolic function

Karst caves are gradually formed due to the karst processes (such as dissolution, erosion, transportation and deposition, etc.). They are mainly distributed along the Mediterranean coast, Eastern Europe, the Middle East, South China, Southeast Asia, as well as in the southeast of the world and Central America[1]. The karst landforms in China are mainly distributed in the southwest provinces such as Yunnan, Guangxi and Guizhou (about 550,000 km^2)[2]. The karst caves are dark, with low temperatures, high humidity and oligotrophic[3] (TOC < 2 mg/L), and organic matter in caves is mainly brought in by air, flowing water, cave-dwelling animals and human visitors[4]. The number of microbial cells in the rocks inside caves can reach 10^6 g^{-1}, and the microbial resources are abundant and the groups are unique[3], which has potential research and application value.

Since the early twentieth century, researchers began to study cave microorganisms and their mineral formation processes, and proposed a classification scheme for the genesis of cave stalactites. Current research on cave microorganisms mainly focuses on the metabolic cycles in biogeochemical and biomineralization processes[3,5], carbonate deposition and dissolution[5–7], as well as the characteristics of microbial communities within cave[8]. As the driving mechanism and environmental response of microorganisms in the material cycle, the sulfur-oxidizing bacteria (Thiohalomonadales) in the Movile Cave[9] cultured the primary productivity of the cave by coupling sulfur oxidation and carbon fixation. Chen et al.[10] discovered in Heshang Cave in Hubei Province that methanotrophs (such as the USCγ bacterial community) acted as methane sinks, consumed methane in the cave and regulated the carbon source balance. During the nitrogen cycle, Thaumarchaeota (ammonia oxidation) and *Nitrospira* (nitrite oxidation) in this cave co-worked together to complete the nitrification. Research on the regulatory mechanism of microorganisms in biomineralization had revealed that, in Baeg-nyong Cave[11],

[1]College of Resources and Environmental Engineering, Key Laboratory of Karst Georesources and Environment, Ministry of Education, Guizhou University, Guiyang 550025, Guizhou, China. [2]Changjiang Survey, Planning, Design and Research Co., Ltd., Wuhan 430019, Hubei, China. [3]Guizhou Karst Environmental Ecosystems Observation and Research Station, Ministry of Education, Guiyang 550025, Guizhou, China. ✉email: ycli3@gzu.edu.cn

microorganisms influenced the cave microenvironment (pH and soil organic matter content) through their metabolic activities. These microorganisms not only included the deposition of carbonate minerals, such as calcite, but also contributed the formation of secondary minerals, including moonmilk and Stalactite. In the Frassasi Cave (acidic)[12], microorganisms (*Acidithiobacillus* and *Ferroplasma*) could generate sulfuric acid/organic acids through sulfur oxidation/metabolism, thereby accelerating rock dissolution and influencing the cave development process. In the respect of characteristics of cave microbial communities, Park et al. found that the microbial groups in dry and moist moonstones were significantly different[11]. While Havlena et al. discovered a large number of unique groups (such as *Metallibacterium* and *Mycobacteria*) serving as functional carriers in caves[12]. Both proved found that the distribution of dominant cave groups had obvious habitat specificity. Concerning the interfering effects of human activities on cave microorganisms, Alonso et al.[13] and Bontemps et al.[14] discovered in Lascaux Cave that tourism led to a decrease in cave microbial diversity (a decrease in the abundance of Euryarchaeota and Woesearchaeota) and a replacement of dominant groups (an increase in the abundance of Bacteroidetes). Rachid and Gungor[15] also found that human entry led to a decrease in the abundance of Thermoplasmata and γ -Proteobacteria, while an increase in the abundance of Bacillus. Biagioli et al.[8] found that exogenous organic matter brought in by human activities enhanced the metabolic function of microorganisms (such as *Chryseobacterium* and *Pseudomonas*) to be heterotrophic. In conclusion, human activities (especially tourism development) could exert a significant impact on the microbial communities in caves.

In this study, sediments in the colored lantern area with tourists (the affected) and the underground primitive dark river area (the unaffected) within the Dushan Tian Cave in Guizhou were sampled and studies. By physicochemical analysis and metagenomic technology, this paper explored the differences in diversity, community structure and metabolic functions of bacteria, fungi and archaea under the influence of human activities. It is expected to provide a basis for the management and protection of karst caves, as well as the development and utilization of cave microorganisms.

Materials and methods

Study area, sample collection and preservation

The sediment samples were collected from Dushan Tian Cave in Guizhou Province (N25°42′35″–25°43′22″, E107°34′25″–107°35′00″). This cave is located in Xiufeng Village, Dushan County, Qiannan Buyei and Miao Autonomous Prefecture, Guizhou Province. It has a subtropical humid monsoon climate. The altitude of the cave body is 762–800 m, with an average annual temperature of 15 °C. The total length of the cave detected is 5437 m. It has two layers of caves and spreads out in a "Y" shape from north to south.

On February 16, 2023, cave sediments were collected along seven locations (D1–D7, Fig. 1) inside the cave. In a five-point sampling method, five points were collected at each of D1–D7 (3 × 3 m, 100 g of sediment 20 cm thic from each point). Method referenced to Bervoets and Addo-Bediako[16], Wang et al.[17] and Palazo et al.[18]. Sediments were sampled and thoroughly mixed in the respective sampling bag, and divided into two portions using self-sealing bags and stored in dry ice buckets for the laboratory. One part was used for physicochemical analysis (be stored in a refrigerator at 4 °C and assayed within one week), and the other was used for DNA extraction and metagenomic analysis (stored in a freezer at − 80 °C). Before sampling, gloves, masks, shoe covers, protective suits and sampling tools (polyethylene sealed bags, tweezers, shovels, centrifuge tubes) were clean and sterile, and each was replaced with the new. During sampling, impurities such as stones, plant residues and animal feces were removed (only fine particle sediments were left). After sampling, the sealed samples were not opened again before physicochemical analysis and microbiological testing. D7 (undeveloped area, 467 m away from the cave entrance, Fig. 1b) had no tourism facilities or visitor and was defined as the underground river area. And D1–D6 (core tourist routes, 21–262 m away from the cave entrance, Fig. 1b) were defined as the colored lantern area due to the tourist activities and lantern lighting.

Physicochemical analysis of the samples

Air dried samples (5 g) from 2 to 0.15 mm were sieved respectively into 50 mL centrifuge tubes. Added 12.5 mL of CO_2-free water (water-to-sedimentation ratio 5:1) respectively, which were then stirred (1 min) and stood (30 min). The pH value and conductivity of 2 mm sample were determined respectively by using a pH meter (PHS-3 C, China) and a conductivity meter. The 0.15 mm sample (4500 r/min, 5 min) was centrifuged and the supernatant was measured for other physicochemical indicators. In the entire process, plastic or agate tools was used. The containers (aluminum boxes, digestion tanks, beakers) were soaked in 10.00% nitric acid (24 h), washed (with deionized water), and dried. Both soil organic matter (SOM) and total organic carbon (TOC) were determined in a titration method (NY/T 1121.6–2006.6). Total nitrogen (TN) and total phosphorus (TP) were determined respectively in an automatic nitrogen determination method (NY/T 1121.24–2012.24) and by the alkali melting-molybdenum antimony anti-spectrophotometer (HJ/T 632–2011). Sulfide (S^{2-}) and sulfate (SO_4^{2-}) were determined by methylene blue spectrophotometry (HJ 833–2017) and titration (NY/T 1121.18–2006.18), respectively. Ammonia nitrogen (NH_4^+), nitrate (NO_3^-) and nitrite (NO_2^-) were all determined by spectrophotometer (T2600, Shanghai Youke, China). Metals such As copper (Cu), manganese (Mn), arsenic (As), chromium (Cr), and iron (Fe) were determined by aqua regia extraction-inductively coupled plasma mass spectrometry (HJ803-2016).

Metagenomic analysis

Samples were thaw at 4 °C, mixed well, and grind in an aseptic condition through a 2 mm sieve. Impurities like carbonates and humic acid were removed with hydrochloric acid (0.1 M, 10 min), and 10.00%PVPP (polyvinylpyrrolidone), respectively. The resides were shaken (30 min) and centrifuged (8000 r/m, 10 min) to enrich microorganisms, maintaining aseptic and anti-contamination throughout the process. Total

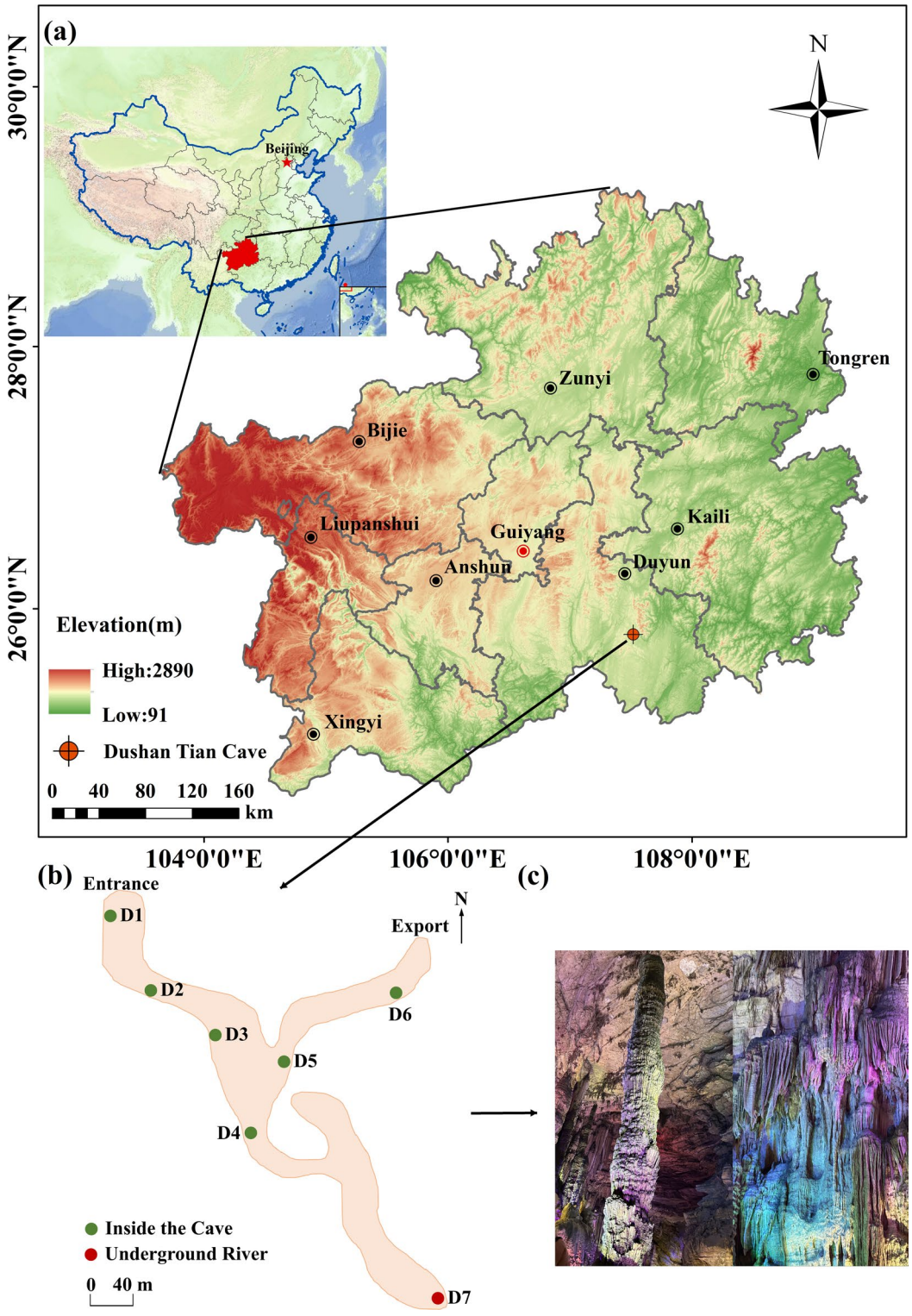

Fig. 1. (**a**) Administrative region map of China, this map is based on the standard map with review number GS (2023)2766 downloaded from the standard map service website of the Ministry of Natural Resources[19], and the base map has not been modified. The enlarged red aera represents the represents the administrative region map of Guizhou Province, this map is based on the standard map with review number GS (2019)3333 downloaded from the standard map service website of the Ministry of Natural Resources[20], and the base map has not been modified. The red coordinates in the lower right corner indicate the specific location of the Dushan Tian Cave in Guizhou. The coordinate information of each municipal city and cave is all sourced from Baidu Maps of China. (**b**) Distribution of sampling points for cave sediments. (**c**) Real scene of the sediment inside the cave. This image was captured by the author "Meiqi Zhang" and had been obtained with the author's consent.

deoxyribonucleic acid (DNA) from sediment microorganisms was extracted using the Fast™ DNA Spin Kit for Soil (MP Biomedicals, CA). The purity and concentration of the extracted DNA were subsequently assessed using an ultramicro spectrophotometer (Thermo Fisher Scientific, NanoDrop2000, USA) and a Fluorometer (QuantusTM Fluorometer, Picogreen). Enzyme-free ultrapure water was used as a substitute and the same extraction steps mentioned above were repeated. DNA integrity of an appropriate amount of sample was subjected to electrophoresis detection (JY600C electrophoresis apparatus, China) using 1.00% agarose gel (Thermo Scientific, USA). DNA being sheared to 350 bp fragments using a Covaris M220 instrument. A PE library was constructed using NEXTFLEX® Rapid DNA-Seq (Bioo Scientific, USA). Finally, metagenomic sequencing was performed using the Illumina NovaSeq6000 platform (Illumina, USA) sequencing platform. The original sequencing data were submitted to NCBI (https://www.ncbi.nlm.nih.gov/#!/landingpage , login number was PRJNA1307558, and it was officially released on September 17, 2025).

Data analysis

The quality sequences were cutting used Fastp (https://github.com/OpenGene/fastp, version 0.23.0), and removed contaminating reads used BWA (http://bio-bwa.sourceforge.net, version 0.7.9a). The original sequencing data for each sample and the cleaned data after quality control were summarized (the optimized sequence) in Table S1. Subsequently, the sequences were stitched and assembled used MEGAHIT (https://github.com/voutcn/megahit, version 1.1.2). The amnio acid sequence were obtained through prediction and translation with Prodigal (https://github.com/hyattpd/Prodigal, version 2.6.3). Redundant gene sets were built used CD-HIT (http://www.bioinformatics.org/cd-hit/, version 4.6.1), aligned with reads (95.00% identity) and quantified for gene abundance used SOAPaligner[21] (http://soap.genomics.org.cn/, version 2.21). Concurrently, species taxonomy and KEGG function annotations were used Diamond (http://www.diamondsearch.org/index.php, version 0.8.35), with details on species and KEGG function abundances provided in supplementary information in Supplementary Material 1.

The raw data were processed used Excel (https://www.microsoft.com/zh-cn/microsoft-365/excel, version 2016), and statistics analysis were conducted to determine the *P* value used IBM SPSS Statistics (https://www.ibm.com/products/spss-statistics, version 25). Veen diagram was generated used BioLadder (https://www.bioladder.cn/web/, version 2.0). The relative abundance chart of microorganisms, principal component analysis (PCA) chart, correlation heat map and metabolic function abundance chart drew used Origin (https://www.originlab.com/, version 2021). Redundancy analysis (RDA) figure drew used TUTU (http://cloudtutu.com/).

Results

Physicochemical properties of sediment samples

The physicochemical properties (Table 1) showed that the study area was weakly alkaline to alkaline (7.51–9.11), with the lowest value occurring on D1 (7.51). Comparison revealed that the concentrations of Sulfide (S^{2-}, abbreviated as SF,1.25 mg/kg DW, $P<0.001$) and ammonia nitrogen (NH_4^+, 10.81 mg/kg DW, $P<0.001$) in the underground dark river area were more six times higher than those in the lantern area. The concentrations of total phosphorus (TP, 213.46 mg/kg DW, $P<0.05$), nitrate (NO_3^-, 13.48 mg/kg DW), copper (Cu, 6.66 mg/kg DW), and chromium (Cr, 23.31 mg/kg DW, $P<0.05$) in the underground dark river area were lower than those in the lantern area. While soil organic matter (SOM), total organic carbon (TOC), sulfate (SO_4^{2-}), and nitrite (NO_2^-) were in the low value range. The first two principal components of PCA (Fig. S9, $P<0.05$) were expressed together up to 70.90% (> 60.00%) of the total variance.

Samples	D1	D2	D3	D4	D5	D6	D7
pH	7.51	8.34	8.66	9.11	8.90	8.40	8.54
EC (us/cm)	3440.00	729.00	1168.00	134.90	111.50	1775.00	103.80
SOM (g/kg DW)	78.14	94.46	5.59	7.68	3.90	5.43	23.88
TOC (g/kg DW)	45.33	54.79	3.24	4.45	2.26	3.15	13.85
TN (mg/kg DW)	5565.46	2414.22	266.74	308.33	46.15	597.11	666.01
TP (mg/kg DW)	24283.72	1973.42	1243.60	2679.93	2694.90	1751.14	213.46
SF (mg/kg DW)	0.54	0.29	0.19	0.41	0.32	0.28	1.25
SO_4^{2-} (mg/kg DW)	4.58	1.15	2.86	0.19	0.38	7.09	0.19
NH_4^+ (mg/kg DW)	4.79	1.51	2.60	1.20	0.44	5.40	10.81
NO_3^- (mg/kg DW)	7487.50	2402.90	195.17	68.09	23.78	104.79	13.48
NO_2^- (mg/kg DW)	54.71	45.39	36.40	1058.98	39.37	32.87	114.87
Cu (mg/kg DW)	151.92	75.56	22.55	24.93	31.85	18.25	6.66
Mn (mg/kg DW)	1799.90	585.54	782.21	473.76	862.24	546.05	483.03
As (mg/kg DW)	19.45	8.44	17.08	9.54	23.44	10.29	9.17
Cr (mg/kg DW)	191.99	37.62	148.33	54.59	118.13	46.49	23.31
Fe (mg/kg DW)	25,213.60	10,907.03	19,959.13	12,353.83	35,218.82	14,596.17	18,307.95

Table 1. Physicochemical properties of sediments in the Dushan Tian Cave, Guizhou (D1–D6: The colored lantern areas affected by human activities. D7: The underground dark river area unaffected by human activities.).

Samples	Ace	Chao1	Shannon	Simpson	Coverage
D1	20,025	20,025	5.654232	0.023583	1
D2	16,121	16,121	5.201304	0.028907	1
D3	18,794	18,794	5.010128	0.038525	1
D4	20,021	20,021	5.061699	0.028364	1
D5	20,353	20,353	5.003275	0.033913	1
D6	19,588	19,588	4.982643	0.035419	1
D7	12,294	12,294	4.472233	0.047071	1
P value	0.002	0.002	0.002	0.004	\

Table 2. The α-diversity and richness index of microbial communities in sediments of Dushan Tian Cave in Guizhou (Ace, Chao1: Richness of the species. Shannon, Simpson: Diversity of the species (including evenness). The four indices belong to the α diversity index.).

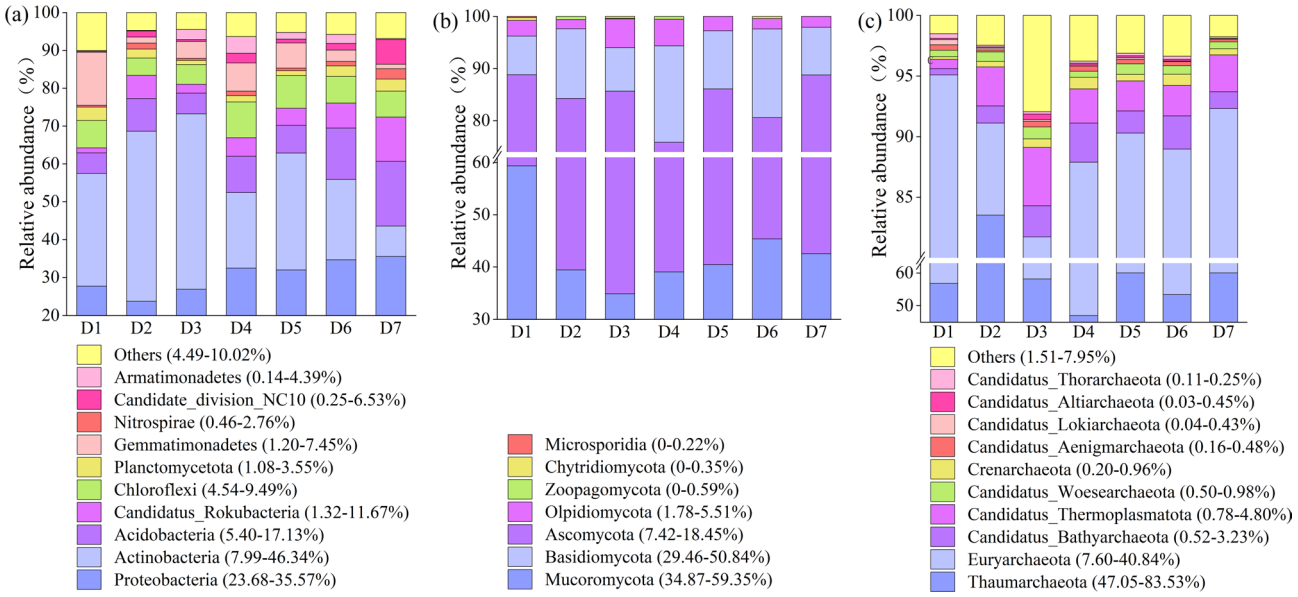

Fig. 2. The structure of the top ten microbial communities in relative abundance in the cave sediments of Dushan Tian Cave in Guizhou at a level of Phylum. (**a**) Bacteria, (**b**) Fungi, (**c**) Archaea. "%" stands for "% relative abundance".

Richness and α diversity of microbial communities in sediment

After quality control of the sediment samples, the effective sequence readings exceeded 98% (Table S5). Meanwhile, combined with core indicators such as the total raw reads (Table S5), the length of the assembled N50 and the contig counts (Table S2), and the gene prediction results (Table S3), it indicated that the sequencing in this study was effective[22]. In Compared on the fungal and archaeal communities (Table S4), the bacterial community exhibited higher Ace, Chao1 and Shannon indices, while the Simpson index was lower. The α diversity index of the fungal community was consistently lower than that of the archaeal community. By comparison, the ranking of species richness within the microbial community was bacteria > archaea > fungi, whereas the ranking of species diversity (including evenness) was Bacteria > Fungi > Archaea. Meanwhile, α -diversity analysis showed that the Ace, Chao1and Shannon indices of D7 were the lowest (Table 2, $P < 0.001$), and the Simpson index was the highest ($P < 0.001$).

Structural composition of microbial communities in sediments

Performed species annotation at the phylum level, Fig. 2a showed that Proteobacteria dominated the bacterial community. The rest included Actinobacteria, Acidobacteria, Candidatus_Rokubacteria and Chloroflexi (> 1.32% relative abundance), etc., and it was observed that the relative abundance of Proteobacteria, Acidobacteria, Candidatus_Rokubacteria, Nitrospirae and Candidate_division_NC10 decreased in the colored lantern area. There were 173 bacterial communities with numerous types of intersections (Fig. 3a). Seven types of fungi were classified (Fig. 2b), and the dominant phyla included Mucoromycota, Basidiomycota and Ascomycota. The relative abundance of Mucoromycota, Ascomycota, Basidiomycota and Olpidiomycota were higher in the colored lantern area, while the community intersections were relatively few (Fig. 3b). In the archaeal community

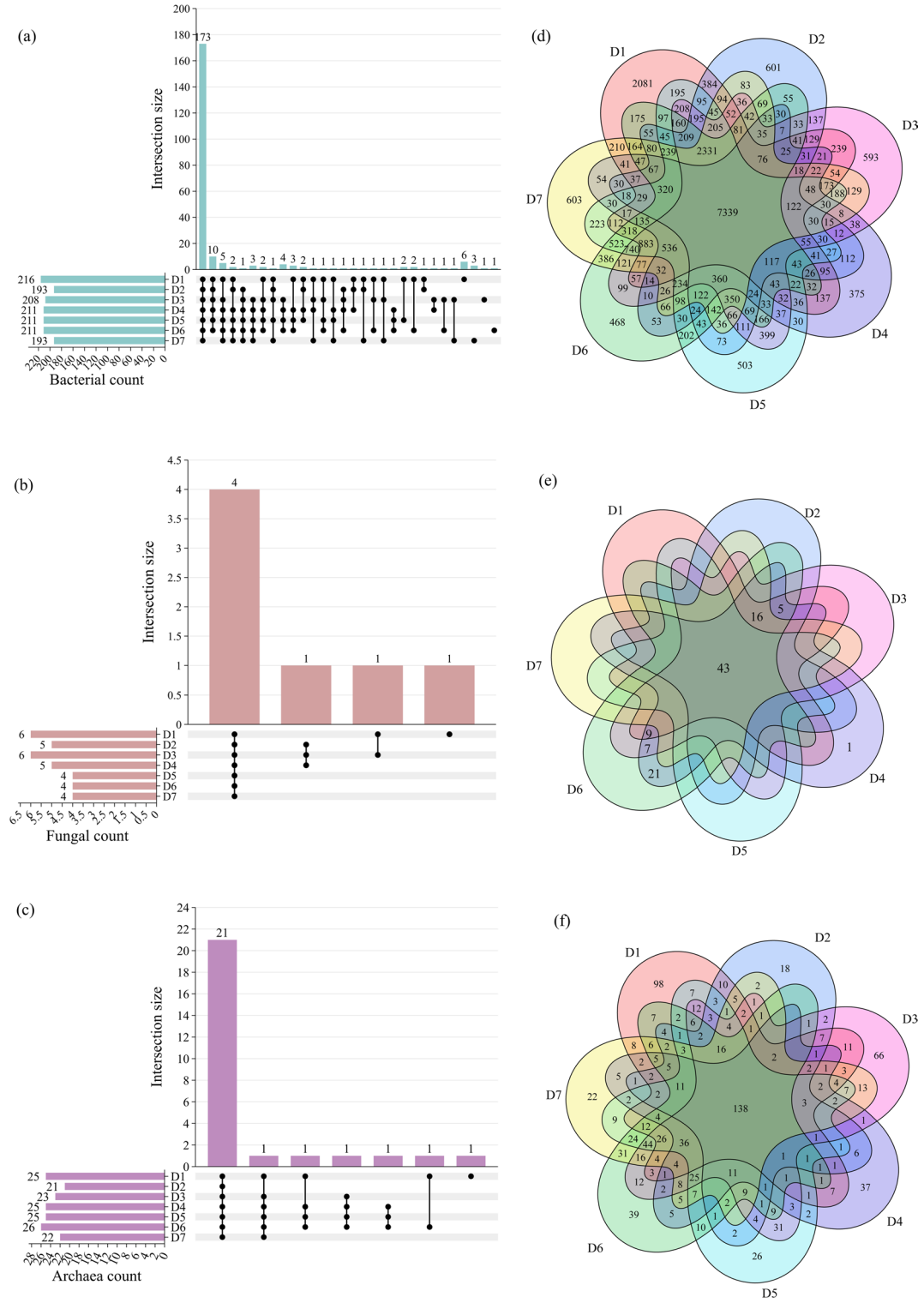

Fig. 3. (**a**–**c**): The intersection of microbial communities in the sediment of Dushan Tian Cave in Guizhou at a level of Phylum, (**d**–**f**): the intersection of microbial communities in the sediment of Dushan Tian Cave in Guizhou at a level of Species, (**a**) and (**d**): Bacteria, (**b**) and (**e**): Fungi, (**c**) and (**f**): Archaea.

(Fig. 2c), Thaumarchaeota and Euryarchaeota were higher (>7.60% relative abundance). In addition, only 21 categories of the intersection archaea communities were observed (Fig. 3c).

At the species level, the bacterial communities include *Carbonactinospora thermoautotrophica* (0.04%–8.04% relative abundance), *Haloactinopolyspora alba* (0.04%–7.97% relative abundance) *and Phytoactinopolyspora halotolerans* (0.05%–3.14% relative abundance) had a high abundance in the colored lantern area (Fig. 4a).

A total of 7339 bacterial species had intersections (Fig. 3d), and the intersections were more numerous in the colored lantern area. In the Fungi communities (Fig. 4b), *Rhizopus_ arrhizus*, *Lipomyces_starkeyi*, and *Olpidium_bornovanus* exhibited high abundances. Then the relative abundance of *Glutinoglossum_americanum*, *Aspergillus_fumigatus* and *Mucor_ambiguus* were high in the underground dark river area. However, the number of intersecting fungal community species was low (Fig. 3e). The relative abundance of *Candidatus Nitrososphaera gargensis*, *Candidatus Nitrososphaera evergladensis*, *Candidatus Nitrosopolaris wilkensis* and *Nitrososphaera viennensis*, etc. in the archaeal community was high (Fig. 4c, relative abundance: > 0.11%, and the first three were candidate species). Among the colored lantern area, the relative abundance of *Candidatus Nitrosotenuis sp. DW1* (relative abundance: < 0.03%, the candidate species) decreased, while *Candidatus Nitrososphaera gargensis*, *Candidatus Nitrososphaera evergladensis*, *Candidatus Methanoperedens nitroreducens* and *Nitrosopumilus ureiphilus* (relative abundance: 0.01%–3.65%, the first three were candidate species) increased. Then the intersection of archaeal communities were three times more than those of fungi (Fig. 3f).

Metabolic functions of microbial communities in sediments

Among the primary metabolic functions of the microbial community (Fig. 5a), the relative abundance of metabolism was higher than 45.00%. Among the secondary metabolic pathways, the relative abundance of the four types of functions, namely Global and overview maps, Carbobydrate metabolism, Amino acid metabolism and Energy metabolism, were high (> 50.00%). In the bacterial community (Fig. S8a), the functional abundance in the colored lantern area was higher than that in the underground dark river area, and it was relatively stable. In the fungal community (Fig. S8b), the functional abundance of Metabolism of cofactors and vitamins was high in the underground dark river area. In the archaea community (Fig. S8c), the underground dark river area lacked Signaling molecules and interaction, and the abundance of the remaining functions was lower than that in the colored lantern area. By comparison, it was found that the microbial functional expression in the underground dark river area was higher (Fig. 5b). The functional expression in the underground dark river area and near the entrance (D2) was higher than that in other lantern areas (D3–D6).

This study was based on KEGG database, and combined with the abundance map of metabolic functions (Fig. 6), the annotation map (Fig. S1–S4) and the gene abundance table (Supplementary Material 4). In the nitrogen metabolism pathway (Fig. 6a), the abundance of "Dissimilatory nitrate reduction" in the underground dark river area was as high as 81.49%, and the abundance of *nirK* and *nosZ* increased. While, the annotation abundance of "Assimilatory nitrate reduction" (*nasA/nasB* and *nirA*) in the colored lantern area was higher. Regarded sulfur metabolic pathways (Fig. 6b), the abundance of "Assimilatory sulfate reduction" (*cysD*, *cysH* and *cysJ* increased) in the colored lantern area increased by 15.23% compared to that in the underground dark river area. In contrast, the abundance of "SOX system" (*soxB* and *soxZ* decreased) decreased by 13.53%. In the carbon metabolism pathway (Fig. 6c), the abundance of "Reductive citrate cycle (Arnon-Buchanan cycle)" (*oorA* and *fumA/FH*), "Pyruvate oxidation" (*pdhD* and *por*) and "Incomplete reductive citrate cycle" (*fumA* and *korA*) in the colored lantern area was lower than that in the underground dark river area. The abundance of "Pentose phosphate pathway (Pentose phosphate cycle)" (*G6PD/zwf*), "Glycolysis (Embden-Meyerhof pathway)" (*glk*, *pfk*, *PGK* and *PK*), "Glyoxylate cycle" (*ACO*) and "Gluconeogenesis" (*TPI* and *PGK*) increased. In the methane metabolism pathway (Fig. 6d), the abundance of "Coenzyme M biosynthesis" (*comC*, *comD* and *comE*) and "Methanogenesis" (*fwdD/fmdD* and *ftr*) in the colored lantern area was decreased. While "Methane oxidation, methanotroph" (*mdh1/mxaF*, *mdh2/mxaI* and *xoxF*) was higher.

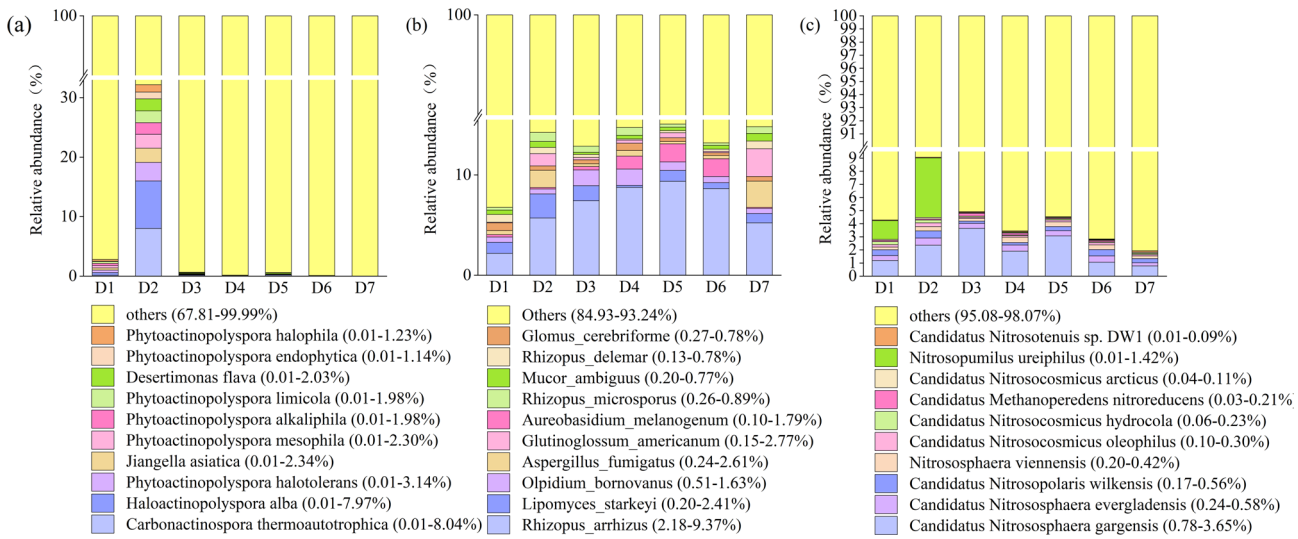

Fig. 4. The structure of the top ten microbial communities in relative abundance in the cave sediments of Dushan Tian Cave in Guizhou at a level of Species, (**a**) Bacteria, (**b**) Fungi, (**c**) Archaea. "%" stands for "% relative abundance".

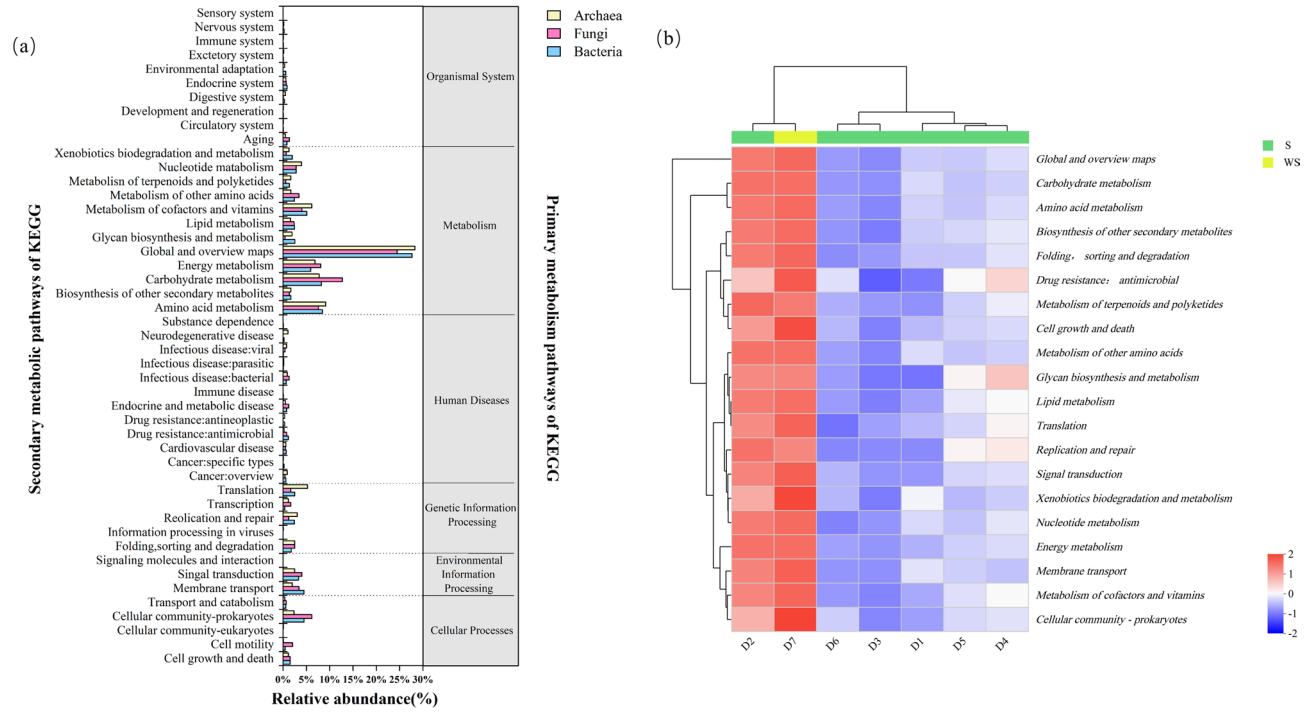

Fig. 5. (**a**) The relative abundance of KEGG primary and secondary metabolic functions of microorganisms in sediments[23,24]. (**b**) Correlation heat map of the secondary metabolic functions of the top 20 microbial communities in terms of abundance in sediments, S: The colored light area affected by human activities, WS: the underground dark river area unaffected by human activities.

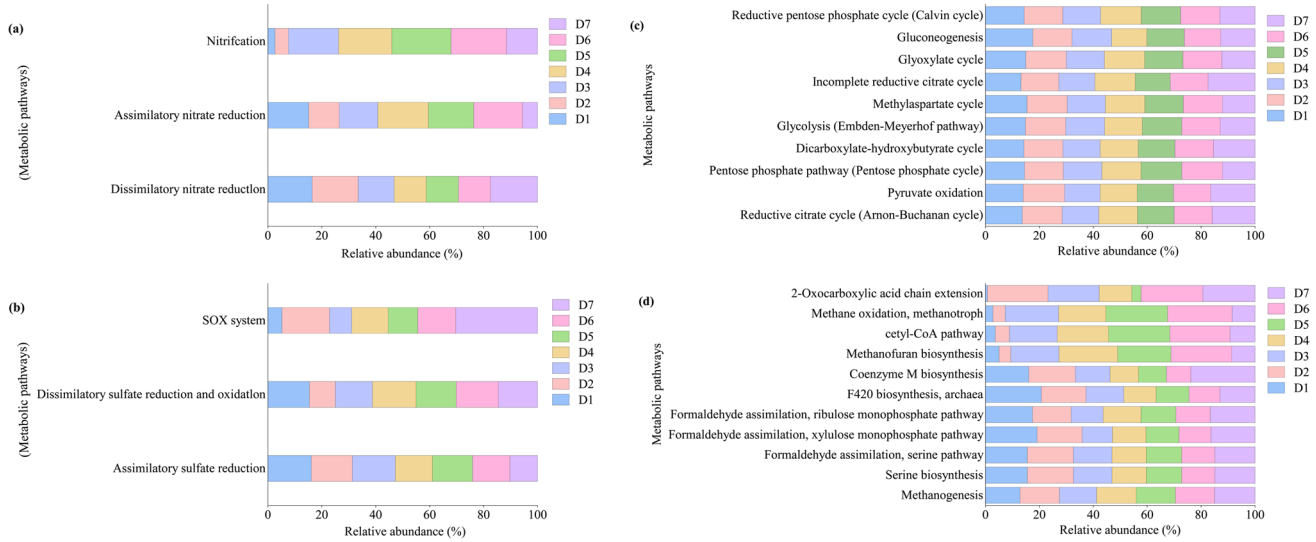

Fig. 6. KEGG annotation abundance map[23,24]. (**a**) Nitrogen metabolism, (**b**) Sulfur metabolism, (**c**) Carbon metabolisms (Top ten), (**d**) Methane metabolism.

Microorganisms and environmental factors in sediments

Through correlation analysis (Fig. 7, Fig. S6) and redundancy analysis (Fig. 7, $P<0.05$), the association between environmental factors and microorganisms in the lantern area was studied. The abundance of Gemmatimonadetes ($R=0.86$) and Microsporidia ($R=0.62$) were significantly positively correlated with TP ($P<0.05$). The abundance of Acidobacteria ($R=-0.82$) and *Rhizopus_arrhizus* ($R=-0.79$) were negatively correlated with SOM and TOC ($P<0.05$). The abundance of *Candidatus_Nitrososphaera_gargensis* ($R=-0.63$) and *Candidatus Nitrosopolaris wilkensis* ($R=-0.75$) was negatively correlated with pH ($P<0.05$). The abundance of Actinobacteria was negatively correlated with SF ($R=-0.75$, $P<0.05$). However, the abundance of *Aspergillus_*

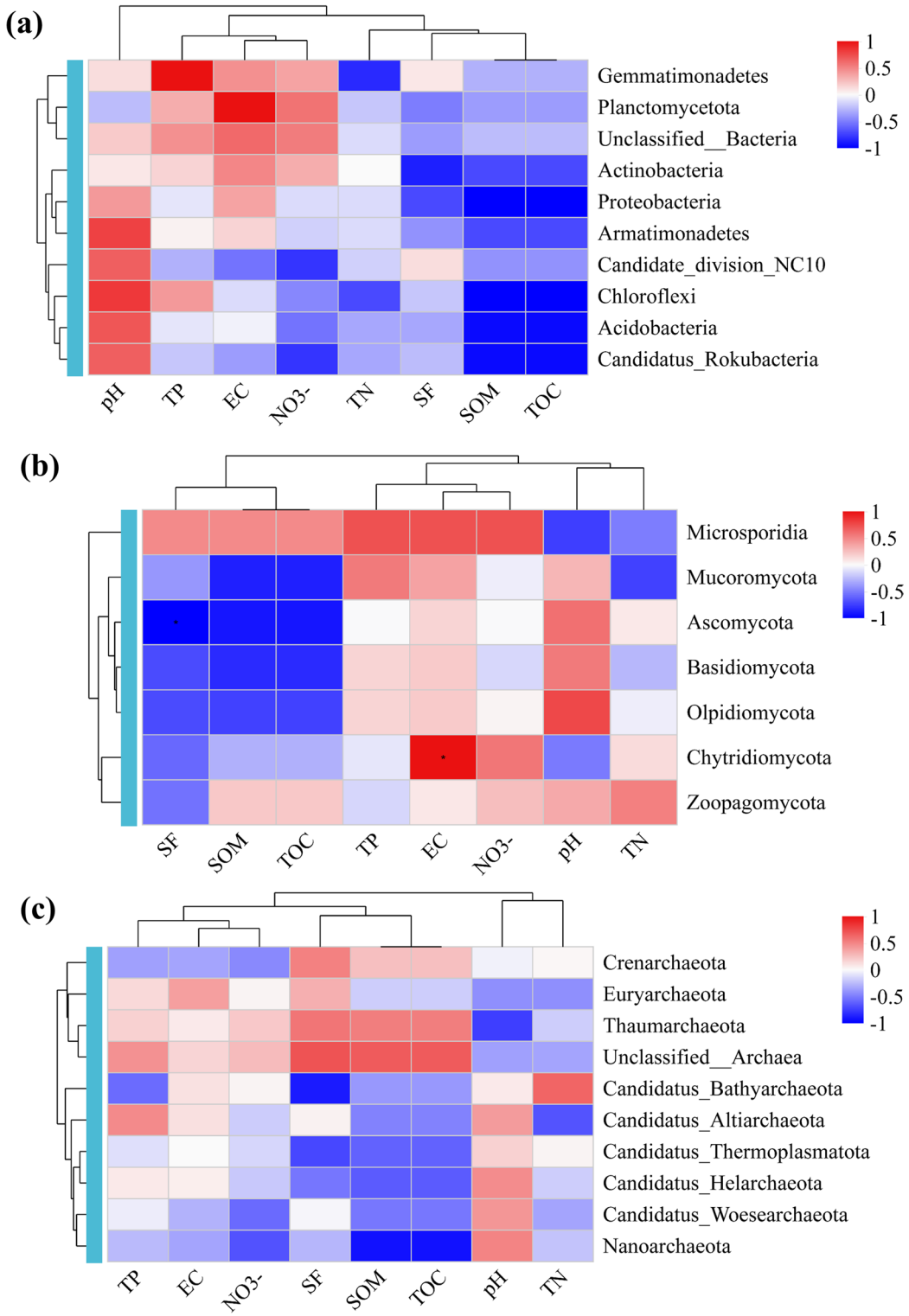

Fig. 7. Heat maps of the correlation between microorganisms and environmental factors in sediments at a level of Phylum, (**a**) Bacteria, (**b**) Fungi, (**c**) Archaea, with R values marked in different colors. The color range of R values is $^{*}P<0.05$, $^{**}P<0.01$, $^{***}P<0.001$.

fumigatus ($R=0.67$) and *Candidatus_Nitrososphaera_ gargensis* ($R=0.71$) were closely positively correlated with Sulfide ($P<0.05$). The direct impact of human activities included disturbances from tourist activities and lanterns, which were timely and localized, directly affected the microbial habitat. Indirect influences referred to a series of environmental changes (pH, SOM, TOC, TP and SF) and caused by direct influence. These indirect effects were characterized by a lag and diffusion, ultimately altered the habitat parameters of microorganisms.

Discussion

This study revealed that the spatial distribution of environmental factors including TP, NH_4^+ and NO_3^-, which were core driving forces behind changes in cave microbial communities, were associated to human activities[25–27], indicated a potential correlation among these variables. But regional variations might be simultaneously influenced by both natural spatial heterogeneity and human activities. Correlation analysis (Fig. 5b) and redundancy analysis (Fig. S10a-b) indicated that the background of phosphorus fertilizers was applied in the agricultural region of Xiufeng Village (Cropland, Fig. S7). This might result in TP concentration in the colored lantern area was 82.85% higher than that in the underground river area (Table 1). It was speculated that the enrichment of Gemmatimonadetes and Microsporidia

was associated with the external input of phosphorus, paralleling the research of Haidău et al.[28]. The abundance of Acidobacteria and *Candidatus_Rokubacteria* in the colored lantern area decreased, probably related the distribution characteristics of exogenous organic matter brought by human activities (Fig. 5a). This trend was similar to the study of Bontemps et al.[29]. The increase in pH within the cave might be attributed to elevated Ca^{2+} levels resulting from limestone dissolution. This chang could further reduced the abundance of *Candidatus_Nitrososphaera_gargensis* in the colored lantern area (Fig. S6), a hypothesis that aligns with the findings of Ai et al.[30]. Furthermore, considering the potential impacts of human activities on hydrogeochemistry and the carbon cycle as reported in existing studies[31], the involvement of Sulfide in the dissolution process of carbonate rocks might be linked to human activities. This associated correspond with the differences in microbial abundance (Gemmatimonadetes and Actinobacteria decreased, *Aspergillus_ fumigatus* and *Candidatus_Nitrososphaera_gargensis* increased) (Fig. 5a, Fig. S6b, c), which was similar with the research results of Biagioli et al.[32]. This study elucidated the effects of both direct human activities and indirect environmental changes, suggested that their contribution could be quantified in the future.

The potential impact of human activities on the key metabolic functions of cave microorganisms was analyzed in conjunction with the abundance of metabolic functions (Fig. 7), gene abundance (Supplementary Material 4), and the structural characteristics of microbial communities.

For nitrogen metabolism pathway, the abundance of the functional genes (*nasA/nasB* and *nirA*) associated with "Assimilatory nitrate reduction" increased, while the functional genes (*nirK* and *nosZ*) related to "Dissimilatory nitrate reduction" decreased in the colored lantern area. This alternation corresponded with the observed trend in regional NO_3^- concentration and the abundance of the relevant bacterial communities for ammonia oxidation and denitrification (*Candidatus Nitrosotenuis sp. DW1* and *Candidatus Methanoperedens nitroreducens*, Table 1; Fig. 4c). According to the studies of Mulec et al.[33] and Zhang et al.[34], certain environmental characteristics, including elevated concentrations of NO_3^-, might be associated with the inhibition of ammonia-oxidizing microorganisms and the enrichment of denitrifying microorganisms. Then the potential denitrification function of the community might be enhanced, and this was related to the potential trend of nitrogen metabolism. This relationship mirrored the research of Albina et al.[35]. We focused only on the association between community structure and nitrogen morphology.

In terms of sulfur metabolic pathway, the regional variations in Sulfide and SO_4^{2-} concentrations observed in the colored lantern area (Table 1) were linked to changes in the abundance of the "Assimilatory sulfate reduction" functional genes (*cysD*, *cysH* and *cysJ* increased). Thus, these findings suggested that regional differences might exist in the functional potential of Sulfide to SO_4^{2-} conversion, a trend that aligns with the research of Wang et al.[36].

In the carbon metabolism pathway, the abundance of functional genes associated with carbon fixation decreased in the colored lantern area, while the abundance of genes related to general carbon metabolism pathway increased. Human activities altered the environmental characteristics in this region, which, in conjunction with the structural differences between carbon fixing related groups (Nitrospirae, *Candidate_division_NC10* and *Candidatus Nitrosotenuis sp. DW1*) and carbon metabolism related groups (Ascomycota, *Rhizopus_arrhizus*, *Lipomyces_ starkeyi* and *Olpidium_bornovanus*). Drawed on the findings of Carney et al.[37] and Xu et al.[38], speculate about the potential role of these communities in the decomposition of exogenous carbon. However, this speculation was only based on the association between gene abundance and commuity structure.

For the methane metabolism pathway, the abundance of functional genes related to methane generation (*fwdD/fmdD* and *ftr*) decreased while the abundance of functional genes related to methane oxidation *(mdh1*, *mdh2* and *xoxF*) increased in the colored lantern area. This shift might be related to the variation in the abundance of the methane oxidation groups (*Candidatus Methanoperedens nitroreducens*) in this region. Referring to the study by Zeng et al.[39], enrichment of methanogenic microorganisms might be inhibited by environmental characteristics related to human activities, which might in turn affect the methane production potential of the community and the balance of the cave's carbon cycle.

This study initially identified a correlation between the environmental characteristics associated to human activities and the structure and functional potential of cave communities. It indicated that the alterations in environmental factors resulted from human activities might influence the material cycling process within the cave ecosystem by modulating the functional genes and community structure of microorganisms. However, due to the constraints of single synchronous sampling, regional openness, and detection conditions, the direct impact of environmental factors had not yet been quantified. The functional analysis, which only based on potential functions predicted by metagenomics, reflected the community patterns observed during the dry season. The conclusion was applicable to the correlation analysis of interference in similar environments, and there might be limitations in the analysis of acid sensitive groups.

Conclusion

This study took Dushan Tian Cave in Guizhou as an example. Through metagenomic sequencing analysis, it was explained that the environmental characteristics related to human activities were associated with the diversity of the cave microbial community, species richness, and the potential of key metabolic functions. Environmental changes included the introduction of exogenous organic matter due to human activities, were associated variations in the abundance of specific microbial groups. These might indirectly influence the biogeochemical cycles of carbon, nitrogen, sulfur and methane within cave ecosystems (nitrogen budget, rock weathering and carbon source balance). In the long term, these associated changes might significantly affect the development of cave landscapes and their bioecological stability. This study offered a regional case for examining microbial responses in cave ecosystems subject to human activity disturbances and enhanced the understanding of the functional potential of cave microorganisms.

Data availability

Authors can provide data upon request. Generated during the current research and the analysis of the data set is available in NCBI website (https://www.ncbi.nlm.nih.gov/) (SRA) found in the repository, landing number is [PRJNA1307558], the web link is [https://dataview.ncbi.nlm.nih.gov/object/PRJNA1307558?reviewer=r9avb35ddks3hq9gfq8iq9ld7h]. We ensure that all data in the manuscript is released on the specified date (September 17, 2025) and that all web links and accesses allow access to public data.

Received: 12 August 2025; Accepted: 25 March 2026
Published online: 04 April 2026

References

1. Voarintsoa, N. R. G., Ratovonanahary, A. L. J., Rakotovao, A. Z. & Bouillon, S. Understanding the linkage between regional climatology and cave geochemical parameters to calibrate speleothem proxies in Madagascar. *Sci. Total Environ.* **784**, 147181. https://doi.org/10.1016/j.scitotenv.2021.147181 (2021).
2. Yi, X. et al. Characteristics and influencing factors of farmland abandonment in the karst rocky desertification area of southwest China. *Ecol. Indic.* **160**, 111802. https://doi.org/10.1016/j.ecolind.2024.111802 (2024).
3. Zhu, H., Jiang, C. & Liu, S. Microbial roles in cave biogeochemical cycling. *Front. Microbiol.* **13**, 950005. https://doi.org/10.3389/fmicb.2022.950005 (2022).
4. Moldovan, O. T. et al. Management of water bodies in show caves—a microbial approach. *Tour Manag.* **78**, 104037. https://doi.org/10.1016/j.tourman.2019 (2020).
5. Zhu, H., Jiang, C. & Liu, S. Microbial roles in cave biogeochemical cycling. *Front. Microbiol.* **13**, 950005. https://doi.org/10.3389/fmicb.2022.950005 (2022).
6. Liu, X. et al. Nitrate determines the bacterial habitat specialization and impacts microbial functions in a subsurface karst cave. *Front. Microbiol.* **14**, 1115449. https://doi.org/10.3389/fmicb.2023.1115449 (2023).
7. Addesso, R. et al. Vermiculations from karst caves: The case of pertosa-auletta system (italy). *Catena* **182**, 104178. https://doi.org/10.1016/j.catena.2019.104339 (2019).
8. Biagioli, F. et al. Microbial diversity and proxy species for human impact in Italian karst caves. *Sci. Rep.* **13**, 689. https://doi.org/10.1038/s41598-022-26511-5 (2023).
9. Chiciudean, I. et al. Competition-cooperation in the chemoautotrophic ecosystem of Movile cave: First metagenomic approach on sediments. *Environ. Microbiol* **17**, 18. https://doi.org/10.1186/s40793-022-00438-w (2022).
10. Cheng, X. et al. Methanotrophs dominate methanogens and act as a methane sink in a subterranean karst cave. *Sci. Total Environ.* **892**, 164562 (2023).
11. Park, S. et al. Microbial diversity in moonmilk of Baeg-nyong cave, Korean CZO. *Front. Microbiol.* **11**, 613. https://doi.org/10.3389/fmicb.2020.00613 (2020).
12. Havlena, Z. E. et al. Microbial ecology of acidic, biogenic gypsum: Community structure and distribution of extremophiles on freshly formed and relict sulfate deposits in a hydrogen sulfide-rich cave. *Appl. Environ. Microbiol.* **91**, e1325–e1397. https://doi.org/10.1128/aem.01397-25 (2025).
13. Alonso, L. et al. Anthropization level of Lascaux cave microbiome shown by regional-scale comparisons of pristine and anthropized caves. *Mol. Ecol.* **28**, 3383–3394. https://doi.org/10.1111/mec.15144 (2019).
14. Bontemps, Z., Hugoni, M. & Moenne-Loccoz, Y. Microscale dynamics of dark zone alterations in anthropized karstic cave shows abrupt microbial community switch. *Sci. Total Environ.* **862**, 13. https://doi.org/10.1016/j.scitotenv.2022.160824 (2023).
15. Rachid, N. A. & Gungor, N. D. Major impacts of caving activities on cave microbial diversity: Case study of Morca cave, Turkey. *Int. Microbiol.* **26**, 179–190 (2023).
16. Addo-Bediako, A. Comparative spatial assessment of trace metal(loid) pollution in the sediments of the lower Olifants River basin in South Africa. *Front. Environ. Sci.* **10**, 11. https://doi.org/10.3389/fenvs.2022.882393 (2022).
17. Wang, J. et al. Assessment of surface sediment properties and heavy metal contamination in typical urban areas of the Yellow River, China. *Sci. Rep.* **15**, 10. https://doi.org/10.1038/s41598-025-87503-9 (2025).
18. Palazon, L. et al. Comparing catchment sediment fingerprinting procedures using an auto-evaluation approach with virtual sample mixtures. *Sci. Total Environ.* **532**, 456–466. https://doi.org/10.1016/j.scitotenv.2015.05.003 (2015).
19. Resources, S.M.S.S. Map of administrative regions in China. http://bzdt.ch.mnr.gov.cn/browse.html?picId=%224o28b0625501ad13015501ad2bfc2191%22. Accessed 17 Aug 2025 (2023).
20. Resources, S.M.S.S. Map of administrative regions of Guizhou Province in China). http://bzdt.ch.mnr.gov.cn/browse.html?picId=%224o28b0625501ad13015501ad2bfc0182%22. Accessed 17 Aug 2025 (2019).
21. Li, R., Li, Y., Kristiansen, K. & Wang, J. Soap: Short oligonucleotide alignment program. *Bioinformatics* **24**, 713–714. https://doi.org/10.1093/bioinformatics/btn025 (2008).
22. Abdelmohsen, U. R. et al. Elicitation of secondary metabolism in actinomycetes. *Biotechnol. Adv.* **33**, 798–811. https://doi.org/10.1016/j.biotechadv.2015.06.003 (2015).
23. Kanehisa, M. Toward understanding the origin and evolution of cellular organisms. *Protein Sci.* **28**, 1947–1951. https://doi.org/10.1002/pro.3715 (2019).
24. Kanehisa, M., Furumichi, M., Sato, Y., Matsuura, Y. & Ishiguro-Watanabe, M. KEGG: Biological systems database as a model of the real world. *Nucleic Acids Res.* **53**, D672–D677. https://doi.org/10.1093/nar/gkae909 (2025).
25. Ji, X., Tang, J. & Zhang, J. Effects of salt stress on the morphology, growth and physiological parameters of juglans microcarpa l. *Seedlings Plants.* **11**, 2381 (2022).
26. Jin, J. et al. Elevated atmospheric co 2 alters the microbial community composition and metabolic potential to mineralize organic phosphorus in the rhizosphere of wheat. *Microbiome* **10**, 17. https://doi.org/10.1186/s40168-021-01203-w (2022).

27. Tong, C. et al. Light intensity-regulated glycogen synthesis and pollutant removal in microalgal-bacterial granular sludge for wastewater treatment. *Water Res.* **271**, 9. https://doi.org/10.1016/j.watres.2024.122988 (2025).
28. Haidău, C. et al. A 16s rrna gene-based metabarcoding of phosphate-rich deposits in muierilor cave, south-western carpathians. *Front. Microbiol.* **13**, 877481. https://doi.org/10.3389/fmicb.2022.877481 (2022).
29. Bontemps, Z. et al. Microbial diversity and secondary metabolism potential in relation to dark alterations in paleolithic Lascaux Cave. *NPJ Biofilms Microbiomes* **10**, 121. https://doi.org/10.1038/s41522-024-00589-3 (2024).
30. Ai, J. et al. The diversity of microbes and prediction of their functions in karst caves under the influence of human tourism activities—a case study of Zhijin Cave in southwest China. *Environ. Sci. Pollut. Res.* **29**, 25858–25868. https://doi.org/10.1007/s11356-021-17783-x (2022).
31. Gong, X. et al. Sulfur-oxygen isotope analysis of so42—sources in cave dripwater and their influence on the karst carbon cycle. *Environ. Res.* **240**, 117508. https://doi.org/10.1016/j.envres.2023.117508 (2024).
32. Biagioli, F. et al. Microbial diversity and proxy species for human impact in Italian karst caves. *Sci. Rep.* **13**, 689. https://doi.org/10.1038/s41598-022-26511-5 (2023).
33. Mulec, J., Skok, S. & Pasic, L. Low bacterial diversity and nitrate levels in cores from deep boreholes in pristine karst. *Life* **14**, 13. https://doi.org/10.3390/life14060677 (2024).
34. Zhang, Z. et al. Nitrate application decreased microbial biodiversity but stimulated denitrifiers in epiphytic biofilms on *Ceratophyllum demersum*. *J. Environ. Manag.* **269**, 10. https://doi.org/10.1016/j.jenvman.2020.110814 (2020).
35. Albina, P. et al. Nitrate and nitrite bacterial reduction at alkaline ph and high nitrate concentrations, comparison of acetate versus dihydrogen as electron donors. *J. Environ. Manag.* **280**, 10. https://doi.org/10.1016/j.jenvman.2020.111859 (2021).
36. Wang, R. et al. Impacts of human activities on the composition and abundance of sulfate-reducing and sulfur-oxidizing microorganisms in polluted river sediments. *Front. Microbiol.* **10**, 13. https://doi.org/10.3389/fmicb.2019.00231 (2019).
37. Carney, K. M., Hungate, B. A., Drake, B. G. & Megonigal, J. P. Altered soil microbial community at elevated co2 leads to loss of soil carbon. *Proc. Natl. Acad. Sci.* **104**, 4990–4995 (2007).
38. Xu, M. et al. Elevated co 2 influences microbial carbon and nitrogen cycling. *BMC Microbiol.* **13**, 11. https://doi.org/10.1186/1471-2180-13-124 (2013).
39. Zeng, G. et al. Methane sink of subterranean space in an integrated atmosphere-soil-cave system. *Environ. Res.* **252**, 12. https://doi.org/10.1016/j.envres.2024.118904 (2024).

Author contributions

Meiqi Zhang: Conceptualization (lead), Data curation (supporting), Formal analysis (lead), Investigation (equal), Validation (lead), Visualization (lead), Writing - original draft (lead).Kun Luo: Conceptualization (equal), Funding acquisition (lead), Project administration (equal), Resources (supporting), Supervision (supporting), Writing-review & editing (supporting).Dehua Liu: Conceptualization (equal), Data curation (lead), Formal analysis (equal), Investigation (lead), Methodology (supporting), Validation (supporting).Yancheng Li: Conceptualization (supporting), Funding acquisition (lead), Investigation (supporting), Project administration (lead), Resources (supporting), Supervision (lead), Writing-review & editing (lead).Qian Liu: Conceptualization (equal), Data curation (supporting), Investigation (supporting), Methodology (lead), Validation (supporting), Visualization (supporting).Jiang Li: Conceptualization (supporting), Funding acquisition (supporting), Resources (lead), Project administration (supporting), Supervision (supporting), Validation (equal), Writing-review & editing (supporting).

Funding

This work was supported by the National Natural Science Foundation of China (52560012), the Science and Technology Plan Project of Guiyang City (No. [2024]2–38) and Guizhou Provincial Science and Technology Achievement Transformation Plan Project (Qiankehe Chengguo [2025] Zhongda 103).

Declarations

Competing interests

The authors declare no competing interests.

Additional information

Supplementary Information The online version contains supplementary material available at https://doi.org/10.1038/s41598-026-46434-9.

Correspondence and requests for materials should be addressed to Y.L.